JZUS

Modeling dual-scale epidemic dynamics on complex networks with reaction diffusion processes[*]

Xiao-gang JIN[1], Yong MIN[‡2]

(^{1}*AI Institute in College of Computer Science and Technology, Zhejiang University, Hangzhou 310027, China*)

(^{2}*College of Computer Science and Technology, Zhejiang University of Technology, Hangzhou 310024, China*)

E-mail: xiaogangj@cise.zju.edu.cn; myong@zju.edu.cn

Abstract: The frequent outbreak of severe foodborne diseases (e.g., haemolytic uraemic syndrome and *Listeriosis*) in 2011 warns of a potential threat that world trade could spread fatal pathogens (e.g., enterohemorrhagic *Escherichia coli*). The epidemic potential from trade involves both intra-proliferation and inter-diffusion. Here, we present a worldwide vegetable trade network and a stochastic computational model to simulate global trade-mediated epidemics by considering the weighted nodes and edges of the network and the dual-scale dynamics of epidemics. We address two basic issues of network structural impact in global epidemic patterns: (1) in contrast to the prediction of heterogeneous network models, the broad variability of node degree and edge weights of the vegetable trade network do not determine the threshold of global epidemics; (2) a 'penetration effect', by which community structures do not restrict propagation at the global scale, quickly facilitates bridging the edges between communities, and leads to synchronized diffusion throughout the entire network. We have also defined an appropriate metric that combines dual-scale behavior and enables quantification of the critical role of bridging edges in disease diffusion from widespread trading. The unusual structure mechanisms of the trade network model may be useful in producing strategies for adaptive immunity and reducing international trade frictions.

Key words: Worldwide trade networks, Foodborne diseases, Scale-free networks, Mean-field analysis

doi:10.1631/jzus.C1300243   **Document code:** A   **CLC number:** TP39; R18

1 Introduction

A large body of theoretical literature discusses how network structures may shape the spread of infectious diseases and influence the design of optimal control strategies (Pastor-Satorras and Vespignani, 2001; Eguíluz and Klemm, 2002; Newman, 2002; Gang *et al*., 2005; Colizza *et al*., 2006; 2007; Balcan *et al*., 2009; Rocha *et al*., 2010). Such works usually focus on the network describing direct human interactions (Khan *et al*., 2009; Cauchemez *et al*., 2011); however, recent infection of enterohemorrhagic *Es-*

cherichia coli (EHEC) in Europe (Dolgin, 2011; Frank *et al*., 2011; Kupferschmidt, 2011a; 2011b) and *Listeria monocytogenes* in the United States (Bennet, 2011) poses a new challenge to the established approach, which for several reasons is not an appropriate one to explore such diseases mediated by trade networks. First, trade-mediated epidemics involve indirect interactions between humans and tradable goods (e.g., infected people in Germany diffused EHEC to the environment via waste, and then infected other people by native vegetables) in addition to simple direct human interactions (Khan *et al*., 2009; Cauchemez *et al*., 2011); hence, the classical SIR (susceptible-infectious-recovered) or SIS (susceptible-infectious-susceptible) model cannot handle this behavior (Dolgin, 2011). Second, trade-mediated diseases involve dual-scale processes: proliferation within a country and worldwide diffusion (Dolgin,

2011). The epidemic and immunity mechanisms are completely different between the two processes; for example, import and export quarantine measures are usually more rigorous than measures within the boundaries of countries. Finally, trade is not a simple transportation of materials or goods, but is closely related to international politics, economics, and society (Chase-Dunn *et al.*, 2000); hence, regulation of trade should be more rational and cautious. These new features and uncertainties affect our ability to assess the global behavior of trade-mediated diseases and control their diffusion.

Motivated by these features and challenges, we propose a dual-scale network epidemic model, including the full Food and Agriculture Organization (FAO) of the United Nations database, to study the interplay among network structure and stochastic features of infection dynamics in defining the global diffusion of epidemics. In particular, previous studies have generally focused on the structural analysis of network connections (Khan *et al.*, 2009; Cauchemez *et al.*, 2011), but the network and dynamic models presented here explicitly address the effects of dual-scale activities. Moreover, the distinct pattern and effects of community structures are identified to explain peculiar epidemic phenomena in trade networks. Finally, such a detailed description provides an opportunity to construct an effective strategy to control global epidemics via trade networks.

2 Vegetable trade network heterogeneity

FAO provides a world list of 254 countries and territories with 574 traded agricultural products. Because vegetables have been reported as the most probable vector of EHEC in the outbreak of haemolytic uraemic syndrome in Germany, vegetable production and trade are the focus of this study. The resulting vegetable trade network (VTN) is a dual-weighted graph comprising 254 weighted nodes denoting countries, whose weights are their vegetable production w_i, and 4243 weighted edges, whose weights w_{ij} account for the direct vegetable trade between countries i and j. This data set was compiled by removing nodes with only input or output edges; thus, these nodes cannot transport infectious diseases. The final network contains N=118 nodes and M=3879 edges, accounting for 99% of worldwide vegetable production and trade. According to previous studies, the presence of small-world, heterogeneous topology, and weight distribution in VTN indicates a possible major impact on disease-spreading behavior (Serrano and Boguñá, 2003).

1. A ubiquitous topological character is the so-called small-world property (Watts and Strogatz, 1998; Amaral *et al.*, 2000). In a small-world network, pairs of nodes are connected by short paths, as expected for a random graph. In VTN, 56% of pairs of nodes are connected by two or fewer steps, and the average shortest path between the 118 countries is very short, d=1.76 (small world effect), which is the shortest among all global network models being compared (Newman, 2003; Serrano and Boguñá, 2003; Guimerà *et al.*, 2005; Colizza *et al.*, 2006; Hu and Zhu, 2009) (Table 1). Additionally, some countries that are physically distant are still close to each other in the network, and the diameter of VTN (the largest length of the shortest pathway) is only 4. More generally, d grows logarithmically with the increase of the number of countries in the network (d<$\log N$). In addition to short distance, local clustering is bound up with the small-world property of the complex networks (Guimerà *et al.*, 2005). The clustering

Table 1 Comparison of global complex networks

Network	Type of graph	n	m	Degree distribution	$<k>$	$<d>$	C	R
VTN	Directed	118	3879	$p_k\sim e^{-k/65.75}$	65.75	1.76	0.66	−
WTW	Directed	179	7510	$p_k\sim k^{-2.6}$	83.91	1.80	0.65	−
Internet	Undirected	10 697	31 992	$p_k\sim k^{-2.5}$	5.98	3.31	0.39	−
WWW	Directed	269 504	1 497 135	$p_k\sim k^{-2.1}$	5.55	11.27	0.29	−
ATN	Directed	3880	18 810	$p_k\sim k^{-2.0}$	9.70	4.73	0.62	+
WMTN	Directed	878	7955	$p_k\sim k^{-2.3}$	18.12	3.60	0.40	+

VTN: Vegetable Trade Network; WTW: Worldwide Trade Web; WWW: World Wide Web; ATN: Air Transportation Network; WMTN: Worldwide Maritime Transportation Network. n: total number of vertices; m: total number of edges; $<k>$: mean degree; $<d>$: mean vertex-vertex distance; C: clustering coefficient; R: degree correlation coefficient (+ is positive correlation, and − is negative correlation)

coefficient, C, quantifies the local cliquishness of a network, and is defined as the probability that two countries directly connected to a third country are also directly connected to each other (Newman, 2003). C is typically larger in VTN than in a random graph and other worldwide networks (Table 1).

2. Another topological aspect of epidemics of complex networks is the degree of distribution—the distribution of the number of links of the nodes (Newman, 2003). Many real-world networks (e.g., Internet and metabolic networks) have only some nodes that are significantly more connected than others (Clauset *et al.*, 2009). In VTN, however, the probability distribution that country i has k_i connections (degree of nodes) to other countries exhibits an exponential distribution, $p(k) \sim e^{-k/\mu}/\mu$, with a very large average value, μ=65.75 (Fig. 1a). It is more heterogeneous than other human epidemic networks (e.g., air-transportation networks and social networks) and general worldwide trade webs (Table 1). Non-trade networks exhibit heavy-tail distribution and a relatively low mean degree of each node (Table 1).

Combining the topological analysis of small-world and degree distribution, we can conclude that the VTNs have extra high connecting density (the highest among the worldwide networks listed in Table 1); hence, the epidemics among countries might be barrier free (Kuperman and Abramson, 2001; Newman, 2002; Santos *et al.*, 2005).

3. As a weighted network (Barrat *et al.*, 2004; Gang *et al.*, 2005), the distribution of three parameters, which are closely related to network weights and epidemic dynamics, is considered. The diffusing ratio of vegetables transported from node i is defined as

$$\beta_i = \sum_i w_{ij} \left/ \left(w_i + \sum_j w_{ij} \right), \right. \quad 0 \le \beta_i \le 1. \qquad (1)$$

If all vegetables are consumed within node i, β_i=0; otherwise, β_i=1 (implying that all vegetables are exported). β_i measures the relative strength of two epidemic activities, diffusion and proliferation. Another parameter that describes the diffusion behavior of VTN is
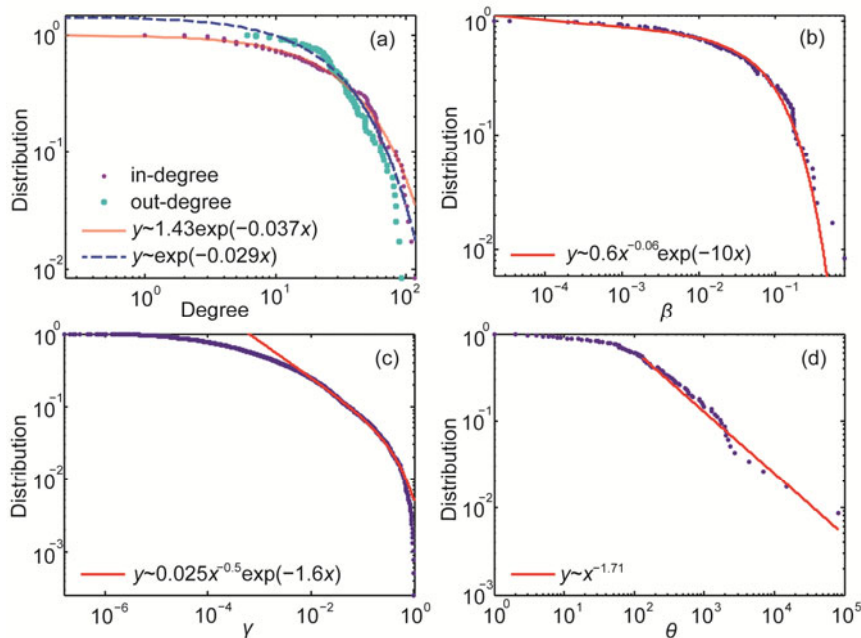
Fig. 1 Degree and weight distribution of the worldwide vegetable trade network
(a) Cumulative in- and out-degree distribution plotted in double-logarithmic scale, with exponential tails. (b–d) Cumulative distribution of three weight-related parameters plotted in double-logarithmic scale, including diffusion ratio β, allotting proportion to neighbor γ, and pathogen volume θ. The fits of γ and θ are focusing on the tail of the data distribution. For all fits, $R^2 > 0.95$. These distributions with exponential or power-law tails illustrate the structural heterogeneity of the vegetable trade network

$$\gamma_{ij} = w_{ij} \Big/ \sum_j w_{ij} \, , \quad 0 \leq \gamma_{ij} \leq 1. \qquad (2)$$

γ_{ij} indicates the allotted proportion of vegetables exported to the direct neighbors of node i. If $\gamma_{ij} \rightarrow 0$, the edge from node i to j is rarely used to transfer pathogens; if $\gamma_{ij} \rightarrow 1$, node j is easily infected when node i has been infected. The pathogen volume of node i is

$$\theta_i = \lceil C \cdot w_i / \min(w_i) \rceil , \quad \theta_i \geq 1, \qquad (3)$$

where C is a scale constant (default is 1). θ_i indicates the upper limit of the number of particles contained in node i, which is closely related to the vegetable production of a country.

The distribution of the three weights is heterogeneous; i.e., most nodes can hold only a few pathogens ($\theta_i < 10$ for 83% nodes) and tend to locally proliferate ($\beta_i \rightarrow 0$), and utilization of most edges is rare (Figs. 1b–1d). Previous studies showed that the heterogeneous distribution of weights might play a positive role in limiting the diffusion of diseases (Gang *et al.*, 2005).

In summary, from the statistical analysis of topological features and weight distribution of VTN, a paradox emerges: the high-density connection pattern could provoke the spread of trade-mediated diseases (Kuperman and Abramson, 2001; Newman, 2002; Santos *et al.*, 2005), while the heterogeneous weight distribution might restrict global epidemics (Gang *et al.*, 2005). To solve the paradox, an explicit dynamic simulation is necessary to clarify the actual role of VTN in disease diffusion.

## 3 Modeling and analyzing dual-scale epidemics

In each Monte Carlo step, we randomly performed reaction and diffusion according to the probability defined in Eqs. (1)–(3). Initial conditions were constructed in a randomly chosen node as the source of diseases and one particle to the node. Transients were discarded and simulations were run long enough so that the initial conditions did not affect the results.

To investigate a solution to the structural paradox and simulate the unique behavior of trade-mediated diseases, a model based on the reaction

diffusion process was developed to study the dynamic behavior of infectious diseases spreading via a dual-weighted VTN (Fig. 2). Reaction diffusion processes generally include particles (representing active disease pathogens) that react locally and diffuse globally (Colizza *et al.*, 2007). In this model, each particle in a node would experience three processes in a discrete time step: extinction, reaction, and diffusion. Initially, a particle goes to extinction with probability $1 - \alpha_i$ (Fig. 2). All nodes are assumed to have the same extinction probability in the model. If a particle survived the extinction process, it can react or diffuse. With probability $1 - \beta_i$, the particle reacts according to the basic reaction scheme

$$A \rightarrow sA . \qquad (4)$$

The coefficient $s = \{2, 3, \dots\}$ indicates the capacity of proliferation; i.e., one particle could proliferate into s new particles. Because the value of s affects only the minimum α for global epidemics, s is fixed to 2 in this model. At any node, the total number of particles cannot exceed pathogen volume θ_i. Particles in node i diffuse to one of its direct neighbors, j, according to probability γ_{ij}. The evolution of the model starts with one particle in a certain node, simultaneously updates the status for each node, and
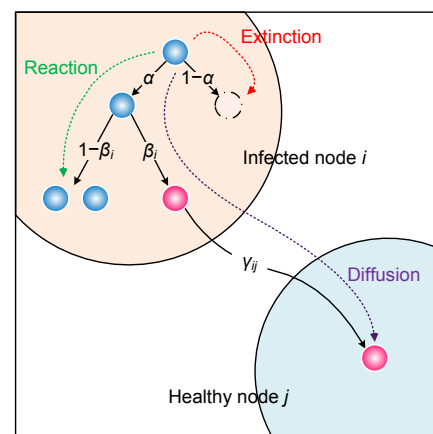
Fig. 2 Reaction diffusion model in networks
Schematic representation of a pathogen particle reacting within an infected node i and diffusing to a healthy node j. Solid arrows represent the probability of corresponding activities; tree dashed lines indicate the full process of extinction (with probability $1 - \alpha$), reaction, and diffusion of a particle. Note that the occupation number of each node can assume any integer value less than pathogen volume θ, as defined in Eq. (3)

finally stops with no surviving particle or all nodes infected. Two indicators of epidemic dynamics can be deduced from the model: the number of evolution steps before all nodes are infected (T), and the proportion of infected nodes at stopping (U). The model meets the requirement of simulating trade-mediated infection (e.g., EHEC) via a VTN for two reasons. First, the reaction diffusion model is analogous to classic models (e.g., SIS and SIR models in Newman (2002)) that hold typical epidemic properties (e.g., phase transition and threshold). Second, the model could distinguish the effect of dual-scale mechanisms in international trade and intra-national production by rationally integrating parameters from both network topology and weights. In the following, the results refer to this specific epidemic model.

For a single node i with one particle, the probability distribution of particles under the extinction, reaction, and diffusion process can be described by two generating functions:

$$f(x) = \alpha x + (1-\alpha), \quad g(x) = (1-\beta_i)x^s + \beta_i. \quad (5)$$

The nest of $f(x)$ and $g(x)$ provides the distribution of particles in node i in one reaction and diffusion:

$$h(x) = f(g(x)) = \alpha(1-\beta_i)x^s + [1-\alpha(1-\beta_i)]. \quad (6)$$

Hence, the distribution of particles in any time step t is t-times iteration of $h(x)$. The average number of diffusing particles is

$$\begin{aligned} D &= \varepsilon + h'(1)\cdot\varepsilon + h'(h(1))\cdot\varepsilon + \cdots \\ &= \varepsilon(1 + h'(1) + (h'(1))^2 + \cdots) \\ &= \frac{\varepsilon}{1-h'(1)} = \frac{\alpha-\alpha(1-\beta_i)}{1-s\alpha(1-\beta_i)}, \end{aligned} \quad (7)$$

where $\varepsilon=\alpha\beta_i$ is the probability that a particle can be diffused. The calculation of D is based on θ_i=inf. Obviously, finite θ_i will reduce the value of D. Considering the classical result of the branching process, the threshold of the model is D=1. Thus, we have

$$\alpha = \frac{1}{1+(s-1)(1-\beta_i)}. \quad (8)$$

For s=2 and $0\leq\beta_i\leq1$, $\alpha_{\min}$=0.5. Therefore, the thresh-

old of our model is closely related to the values of β and θ. Note that the derivation is based on the assumptions that the size of the baseline network is infinite and that the distribution of degree and weights is homogeneous.

Considering node i has k out-edges and allotting proportion is γ_{ij}, j=1, 2, …, k, we can calculate the probability distribution of the number of edges used (i.e., transporting the pathogen particles). When D particles are diffused from node i, the distribution is

$$U_D(x) = \prod_{j=1}^{k} T_j(x), \quad (9)$$

where $T_j(x)=[1-(1-\gamma_{ij})^D]x+(1-\gamma_{ij})^D$. Therefore, the average number of edges used is

$$U_D{}'(1) = k - \sum_{j=1}^{k}(1-\gamma_{ij})^D. \quad (10)$$

When focusing on the situation at the threshold point (D=1), we found $U_1'(1)$=1, which is unrelated to degree k and allotting proportion γ_{ij}. However, these two parameters could affect the epidemic speed when D>1.

If we assign different survival probabilities to the reaction and diffusion process for reflecting different immunity mechanisms in intra- and inter-dynamics, we can map this behavior to the current model. The behavior is: (1) A particle is chosen to react (with probability $1-\beta_i'$) or diffuse (with probability β_i'); (2) When reacting, the particle survives with probability α'; (3) When diffusing, the particle survives with probability α''. This behavior can be described using the current model by redefining the parameters as

$$\alpha = (1-\beta_i')\alpha' + \beta_i'\alpha'', \quad \beta_i = \frac{\beta_i'(1-\alpha'')}{1-\alpha}. \quad (11)$$

Usually, quarantine measures of international trades are usually more rigorous than measures within a country ($\alpha'>\alpha''$); hence, $\beta_i<\beta_i'$. It means that the different survival probabilities will lead to less opportunity for diffusion between different countries. Because the results of this study are based on a power law distribution with cutoff of β_i (Fig. 1), current conclusions are also fit for the situation of different survival probabilities. Therefore, the model could distinguish the behavior of dual-scale mechanisms.

4 Effects of topological and weighted heterogeneity

To ascertain the role of heterogeneous distribution of different structural factors in the spatio-temporal pattern of the epidemic process, the evolution of epidemics obtained from the actual VTN is compared to those obtained from three homogeneous network models providing null hypotheses (Fig. 3). The first model network is the homogeneous diffusion ratio network (HDRN), in which $\beta=0.5$ for all nodes, which means that the proliferation and diffusion of particles are balanced. The second model is the homogeneous allotting proportion network (HAPN), in which $\gamma_{ij}=1/k$ (k is the out-degree of node i), which means that the diffusion is homogeneous for all neighbors. HDRN and HAPN retain the exact topology and other parameters of the actual VTN except for parameters in the homogeneous hypotheses. The third model, homogeneous node degree network (HNDN), is a homogeneous Erdos-Rényi random network with the same N, $<k>$, and β_i as in VTN, and $\gamma_{ij}=1/k$ as in HAPN for each node. In all homogeneous models, the volume of pathogens, θ_i, is equal to that of the real VTN with C=1 (VTN$_1$). We also test the effect of θ_i with a different scaling constant C=0.01 on VTN (VTN$_{0.01}$). The larger C indicates that every country could contain more pathogens, but the proportions of pathogen volumes of different countries are unaltered. The difference between the behavior observed in the homogeneous models and that in actual cases provides striking evidence for a direct relationship between heterogeneous structure and epidemic pattern. The HAPN and HNDN models display the same epidemic threshold and average infected proportion as VTN$_1$. However, a different scenario is observed for HDRN and VTN$_{0.01}$, where the epidemic threshold is significantly larger than that of VTN$_1$ (Fig. 3a). Indeed, the analytical inspection of the epidemic equations shows that the ratios β_i and the volume of pathogens play a critical role in the global diffusion of trade-mediated diseases. Additionally, Fig. 3b reports the average number of evolution steps before all nodes are infected after the epidemic threshold (i.e., convergence time). The homogeneous distribution γ could lead to a higher convergence speed for infecting all nodes, because it avoids the gathering of the output pathogens from a node in a few neighbor nodes. Strikingly, the number of infected nodes and convergence time obtained are both similar for HAPN and HNDN (Fig. 3), indicating that the heterogeneous degree distribution does not affect the overall properties of the epidemic pattern, including the epidemic threshold and speed for global epidemics. The reason might be an extra high average degree (Table 1), by which the effects of heterogeneous connections are shaded (Newman, 2003). Contrarily, β_i and θ_i have significant impact on the threshold and convergence speed of epidemics of VTN. Although previous studies showed that the overall epidemic behavior is determined by heterogeneous inter-connection patterns (Newman, 2002; Gang *et al.*, 2005; Colizza *et al.*, 2006), our dual-scale model emphasizes the critical role of intra-dynamics in determining the epidemic threshold and speed.
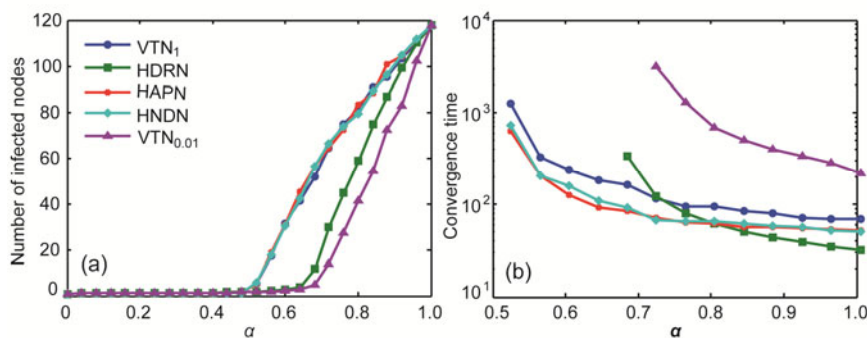
Fig. 3 Phase diagrams of epidemics of the vegetable trade network

(a) Phase transition lines show the average infectious ratio for five network models under different survival probabilities, α; lines indicate the epidemic threshold of network models. (b) Lines illustrate the average number of evolution steps before complete infection of five network models when α is larger than thresholds. VTN$_1$ and VTN$_{0.01}$ have the same original structure and weights of the vegetable trade network but with different pathogen volumes (C=1 and 0.01 in Eq. (3), respectively). HDRN, HAPN, and HNDN represent hypothetic network models with homogeneous diffusion ratio, allotting proportion, and node degree, respectively

More interestingly, although parameters β_i and θ_i have significant impact on the overall epidemic patterns, their behaviors are different. $\text{VTN}_{0.01}$ displays a requirement of a high probability of survival (α) of the epidemics with a long convergence time; however, HDRN shows a high threshold with a short convergence time. Indeed, the rise of β_i or the drop of θ_i could limit the proliferation within nodes and lead to increase in the threshold. A low β_i also enhances the diffusion and raises the epidemic speed. With a large θ_i, the threshold of actual VTN_1 is very close to the theoretical minimum of α (α=0.5 for s=2) to maintain a global infection. This clarifies the paradox between topology and weights; i.e., the dominant effect of the heterogeneous distribution of β_i proves that VTN actually instigates the global spread of infectious diseases. In summary, more attention should be paid to controlling infections within countries rather than global trade patterns. Such strategies could help reduce international trade friction, for example, the argument between Germany and Spain about the EHEC outbreak.

5 Effects of community structure

Community structure—groups of nodes with dense connectivity among them and a lower level of connectivity between groups—is another important feature of complex networks that could limit the transmission of infectious diseases (Kitano, 2004; Variano *et al.*, 2004; Salathé and Jones, 2010). Community structure in VTN is detected using the algorithm proposed by Newman and Girvan (2004) and Newman (2006). The algorithm is rigorous because it maximizes an explicit parameter, called modularity Q, identifies the number of non-overlapping communities, assigns membership to communities, and tests the significance of the results. Usually $Q>0.3$ states the significant existence of communities in the target networks. Feeding VTN with edge weights through the algorithm, the network is divided cleanly into six non-overlapping communities and, remarkably, the maximum modularity reaches 0.492. Moreover, we use a community detection algorithm based on random walk to validate the existence of communities in VTN (Rosvall and Bergstrom, 2008). The results show that the lower

bound of code length (L) of six communities is less than the value of one community, and thus communities exist. In fact, 83% of the total vegetable trade occurs within the six communities. It is similar to the situation of an air transportation network (Guimerà *et al.*, 2005). For example, the community that contains Hong Kong displays a zonal distribution along the coasts of the Pacific and Indian Ocean, and across three continents and 26 countries. Therefore, in VTN, a network community is more accurate in reflecting the trade relationships than the geographical distance.

Unexpectedly, the pattern of community structure in VTN is distinctive from current theoretical hypothesis, which usually assumes that only a few nodes link to outside of a community. In VTN, however, it is found that about 96% nodes have bridging edges (the edges connecting different communities), which suggests that almost all nodes have an opportunity of transporting disease to outside of a community. Moreover, 64% edges of the entire VTN are the bridging edges. Therefore, the connection between different communities in VTN displays a special pattern with dense topology but weak weights. The distinct pattern of community structure implies a peculiar role in global epidemics, and can be used to make more effective strategies to control trade-mediated epidemics.

Community is an effective structural pattern for containing damage and diseases locally to minimize the effects of the whole networks, in order to ensure the robustness of network stability to random perturbation (Kitano, 2004; Variano *et al.*, 2004). Surprisingly, the global spread of infectious diseases is not limited by the existence of communities in VTN. The infection processes within the source community which contains the node with the initial particle, are approximately synchronous with the non-source community and the overall VTN (Figs. 4a and 4b). This implies a failure of the community structure in which pathogens quickly stride over the boundary of the source community and diffuse to other communities across bridging edges. The cross-activity ratio, which is the proportion of particles across community boundaries at each step, is plotted in Fig. 4c. There is a nonlinear change of the number of active bridging edges, from which about 40% transmission is cross-activity in the initial epidemic period (accounting for only 3% of the total epidemic duration), and then the
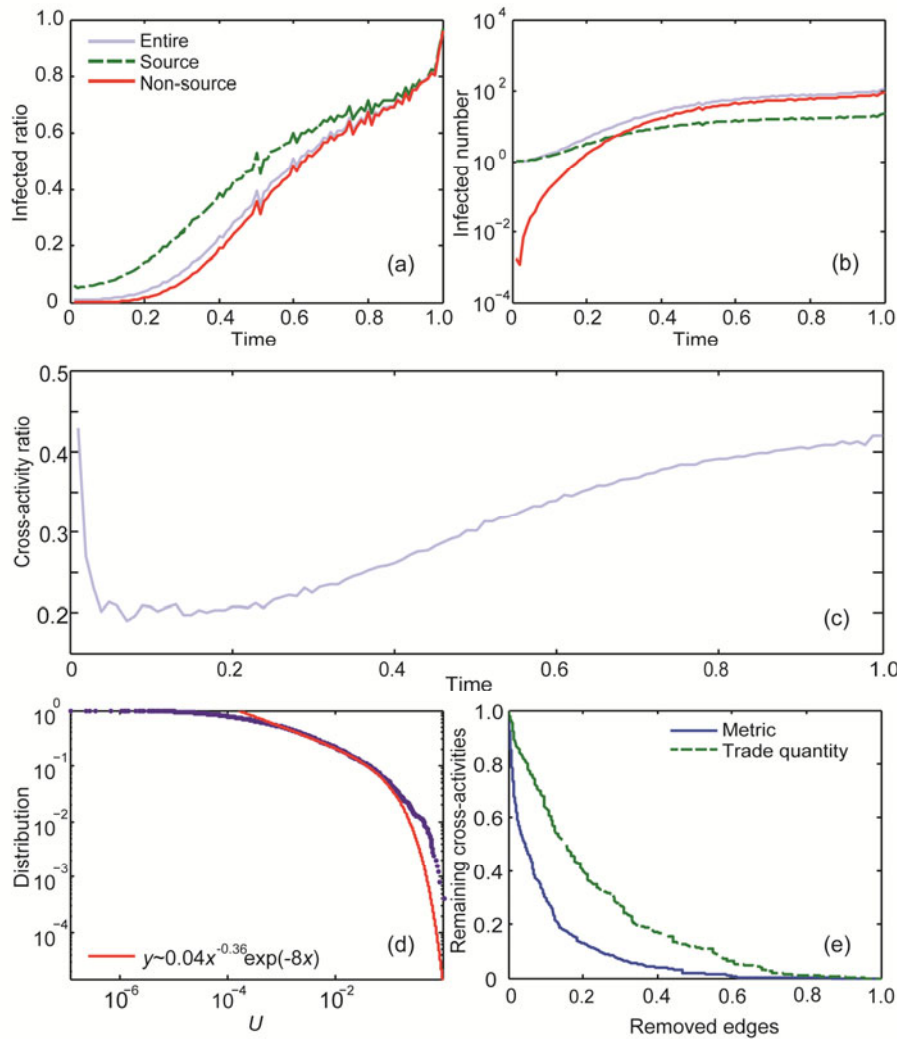
Fig. 4 Community effects on epidemic dynamics
(a, b) Change of the infected ratio and the number of infected nodes of the entire network, source community, and non-source communities. The source community contains the initial pathogen particle, which is randomly chosen from all nodes in simulation. (c) Change of the cross-activity ratio along with the infectious process. The cross-activity is defined as the diffusion between different communities. The time axis in (a)–(c) is normalized to [0, 1], divided by the total number of steps for each simulation. (d) The power law with cutoff distribution of importance of bridging edges, which is quantified by the edge importance defined in Eq. (10). For the fit, $R^2>0.95$. (e) The lines indicate the proportion of remaining cross-activities after knocking out certain edges. The sequence of knockout follows the descending rank of edge importance and trade quantity

cross-activity decreases to ~20%, and finally increases to ~40% at the end of epidemics. This proves that the bridging edges play a critical role in the early stage of global epidemics via VTN. Although community structure fails to limit infection, the existence of bridging edges provides an opportunity to formulate strategies to control global epidemics of trade-mediated diseases.

   To discriminate the role of bridging edges in the spatio-temporal pattern of the epidemic process, we aim to quantitatively analyze the bridging edges for effectively transporting diseases. An infectious process is assumed to start from a node i with one pathogen particle, where an initiative node cannot be infected by other nodes again. At each time step t ($t\geq0$), the average number of exporting particles from node i is provided by $s^{t+1}\alpha^t(1-\beta_i)^{t+1}\beta_i$. Because α is identical among all nodes, we set $\alpha=1$ for simplification. We can therefore define the probability of at least one particle passing through an edge with γ_{ij} before time t

as

$$U_{ij} = \prod_{k=0}^{t} (1 - \gamma_{ij})^{s^{t+1}(1-\beta_i)^{t+1}\beta_i}. \qquad (12)$$

U_{ij} is the function of s, β, and γ; hence, it could integrate the dual-scale epidemic behaviors. We can set a small t (t=5 in this study) for evaluating the edge importance at the early epidemic stage.

Based on U_{ij}, the importance of all bridging edges can be quantified. The cutoff power law distribution (Clauset *et al.*, 2009) of U_{ij} (Fig. 4d) suggests that only a few bridging edges are critical in quickly transporting disease between communities in the early period. Based on the connecting pattern of bridging edges, we find that: (1) Critical bridging edges always transport diseases from small-trade countries (e.g., Belize and Gambia) to large-trade countries (e.g., United Kingdom, France, and Germany); (2) Europe is the primary target of global epidemics, and is susceptible in worldwide trade. This result shows that the outbreak of EHEC in Europe implies an inevitability of globally spreading infectious disease.

Because previous work related communities to stability (Kitano, 2004; Variano *et al.*, 2004), a hypothesis of stability (robustness against the global spread of infectious diseases) was developed by simulating two disturbance scenarios of VTN. In the first scenario, we break bridging edges in descending order of U_{ij}, which could occur with trade control. This disturbance leads to a rapid decrease of cross-activities in the initial epidemic period, in which the cross-activities decrease by 70% after removing 10% most important bridging edges (Fig. 4e). In the second scenario, we break bridging edges according to the trade quantity. In response to this disturbance, the change of the level of cross-activities is more moderate (losing only 38% cross-activities when removing 10% largest quantity trades) (Fig. 4e). Compared with a block of edges with the largest trade quantity, the regulation of identified links is not only more effective but also more economical.

6 Conclusions

This is a system analysis that has been performed for epidemic dynamics of trade, yielding a number of significant results. VTN is a small-world, high-density, and high-cluster heterogeneous network that instigates the global diffusion of diseases. Theoretically, we find that the heterogeneous distribution of degree and weights could not determine the overall epidemic pattern; however, the intra-dynamics is critical in trade-mediated diseases. We also identify the communities in the vegetable trade network and show that the particular connecting pattern between communities cannot be explained based on rare-link hypothesis. Moreover, the vitality of bridging edges leads to the failure of community structures to limit disease diffusion and provides a control strategy, which makes a practical trade-off between cost and efficiency in controlling global diffusion. This study offers an initial approach to understanding the spatial dual-scale epidemic dynamics of trade networks. In the future, temporal multi-scale characteristics should be considered in research on foodborne diseases. In fact, the tourism network plays a real-time role in spreading EHEC, while the role of the trade network is latent, i.e., a slow but durable medium to spread EHEC (Frank *et al.*, 2011). This characteristic makes the behavior of foodborne diseases more complex and mysterious than diffusion processes based solely on a mediated network.

References

Amaral, L.A.N., Scala, A., Barthélémy, M., *et al.*, 2000. Classes of small-world networks. *Proc. Natl. Acad. Sci. USA*, **97**(21):11149-11152. [doi:10.1073/pnas.200327 197]

Balcan, D., Colizza, V., Goncalves, B., *et al.*, 2009. Multiscale mobility networks and the spatial spreading of infectious diseases. *Proc. Natl. Acad. Sci. USA*, **106**(51):21484-21489. [doi:10.1073/pnas.0906910106]

Barrat, A., Barthélemy, M., Pastor-Satorras, R., *et al.*, 2004. The architecture of complex weighted networks. *Proc. Natl. Acad. Sci. USA*, **101**(11):3747-3752. [doi:10.1073/pnas.0400087101]

Bennet, N., 2011. Infectious disease surveillance update. *The Lancet Infect. Dis.*, **11**(11):815. [doi:10.1016/S1473-3099(11)70305-X]

Cauchemez, S., Bhattarai, A., Marchbanks, T.L., *et al.*, 2011. Role of social networks in shaping disease transmission during a community outbreak of 2009 H1N1 pandemic influenza. *Proc. Natl. Acad. Sci. USA*, **108**(7):2825-2830. [doi:10.1073/pnas.1008895108]

Chase-Dunn, C., Kawano, Y., Brewer, B.D., 2000. Trade globalization since 1795: waves of integration in the world-system. *Am. Sociol. Rev.*, **65**(1):77-95. [doi:10.2307/2657290]

Clauset, A., Shalizi, C.R., Newman, M.E.J., 2009. Power-law distributions in empirical data. *SIAM Rev.*, **51**(4):661-703. [doi:10.1137/070710111]

Colizza, V., Barrat, A., Barthélemy, M., *et al.*, 2006. The role of the airline transportation network in the prediction and predictability of global epidemics. *Proc. Natl. Acad. Sci. USA*, **103**(7):2015-2020. [doi:10.1073/pnas.0510525103]

Colizza, V., Pastor-Satorras, R., Vespignani, A., 2007. Reaction-diffusion processes and metapopulation models in heterogeneous networks. *Nat. Phys.*, **3**(4):276-282. [doi:10.1038/nphys560]

Dolgin, E., 2011. As *E. coli* continues to claim lives, new approaches offer hope. *Nat. Med.*, **17**(7):755. [doi:10.1038/nm0711-755]

Eguíluz, V.M., Klemm, K., 2002. Epidemic threshold in structured scale-free networks. *Phys. Rev. Lett.*, **89**(10):108701. [doi:10.1103/PhysRevLett.89.108701]

Frank, C., Werber, D., Cramer, J.P., *et al.*, 2011. Epidemic profile of Shiga-toxin–producing *Escherichia coli* O104:H4 outbreak in Germany. *N. Engl. J. Med.*, **365**(19):1771-1780. [doi:10.1056/NEJMoa1106483]

Gang, Y., Tao, Z., Jie, W., *et al.*, 2005. Epidemic spread in weighted scale-free networks. *Chin. Phys. Lett.*, **22**(2):510-513. [doi:10.1088/0256-307X/22/2/068]

Guimerà, R., Mossam, S., Turtschi, A., *et al.*, 2005. The worldwide air transportation network: anomalous centrality, community structure, and cities' global roles. *Proc. Natl. Acad. Sci. USA*, **102**(22):7794-7799. [doi:10.1073/pnas.0407994102]

Hu, Y., Zhu, D., 2009. Empirical analysis of the worldwide maritime transportation network. *Phys. A*, **388**(10):2061-2071. [doi:10.1016/j.physa.2008.12.016]

Khan, K., Arino, J., Hu, W., *et al.*, 2009. Spread of a novel influenza A (H1N1) virus via global airline transportation. *N. Engl. J. Med.*, **361**(2):212-214. [doi:10.1056/NEJMc0904559]

Kitano, H., 2004. Biological robustness. *Nat. Rev. Genet.*, **5**(11):826-837. [doi:10.1038/nrg1471]

Kuperman, M., Abramson, G., 2001. Small world effect in an epidemiological model. *Phys. Rev. Lett.*, **86**(13):2909. [doi:10.1103/PhysRevLett.86.2909]

Kupferschmidt, K., 2011a. Scientists rush to study genome of lethal *E. coli*. *Science*, **332**(6035):1249-1250. [doi:10.1126/science.332.6035.1249]

Kupferschmidt, K., 2011b. As *E. coli* outbreak recedes, new questions come to the fore. *Science*, **333**(6038):27. [doi:10.1126/science.333.6038.27]

Newman, M.E.J., 2002. Spread of epidemic disease on networks. *Phys. Rev. E*, **66**(1):016128. [doi:10.1103/ PhysRevE.66.016128]

Newman, M.E.J., 2003. The structure and function of complex networks. *SIAM Rev.*, **45**(2):167-256. [doi:10.1137/ S003614450342480]

Newman, M.E.J., 2006. Modularity and community structure in networks. *Proc. Natl. Acad. Sci. USA*, **103**(23):8577-8582. [doi:10.1073/pnas.0601602103]

Newman, M.E.J., Girvan, M., 2004. Finding and evaluating community structure in networks. *Phys. Rev. E*, **69**(2):026113. [doi:10.1103/PhysRevE.69.026113]

Pastor-Satorras, R., Vespignani, A., 2001. Epidemic spreading in scale-free networks. *Phys. Rev. Lett.*, **86**(14):3200-3203. [doi:10.1103/PhysRevLett.86.3200]

Rocha, L.E.C., Liljeros, F., Holme, P., 2010. Information dynamics shape the sexual networks of Internet-mediated prostitution. *Proc. Natl. Acad. Sci. USA*, **107**(13):5706-5711. [doi:10.1073/pnas.0914080107]

Rosvall, M., Bergstrom, C.T., 2008. Maps of random walks on complex networks reveal community structure. *Proc. Natl. Acad. Sci. USA*, **105**(4):1118-1123. [doi:10.1073/pnas.0706851105]

Salathé, M., Jones, J.H., 2010. Dynamics and control of diseases in networks with community structure. *PLoS Comput. Biol.*, **6**(4):e1000736. [doi:10.1371/journal.pcbi.1000736]

Santos, F.C., Rodrigues, J.F., Pacheco, J.M., 2005. Epidemic spreading and cooperation dynamics on homogeneous small-world networks. *Phys. Rev. E*, **72**(5):056128. [doi:10.1103/PhysRevE.72.056128]

Serrano, M.Á., Boguñá, M., 2003. Topology of the World Trade Web. *Phys. Rev. E*, **68**(1):015101. [doi:10.1103/ PhysRevE.68.015101]

Variano, E.A., McCoy, J.H., Lipson, H., 2004. Networks, dynamics, and modularity. *Phys. Rev. Lett.*, **92**(18):188701. [doi:10.1103/PhysRevLett.92.188701]

Watts, D.J., Strogatz, S.H., 1998. Collective dynamics of small-world networks. *Nature*, **393**(6684):440-442. [doi:10.1038/30918]